MICROSTRUCTURE AND MECHANICAL PROPERTIES OF WELDS OF Al – Mg – Si ALLOYS AFTER DIFFERENT MODES OF IMPULSE FRICTION STIR WELDING

S. Yu. Kondrat'ev,[1] Yu. N. Morozova,[1, 2] Yu. A. Golubev,[1, 2] C. Hantelmann,[2] A. A. Naumov,[1] and V. G. Mikhailov[1, 2]

Welded joints of aluminum alloy 6082-T6 formed by the method of impulse friction stir welding are studied. The effect of the power and frequency of the pulses on the microstructure and mechanical properties of the welded joints is determined. Application of an additional pulse during the welding affects the surface quality and the shape of the weld, the distribution of the oxide layer and of particles of the hardening phase, and the grain size in the zone of dynamic recrystallization.

Key words: impulse friction stir welding, power and frequency of pulses, microstructure, mechanical properties, Al – Mg – Si alloy.

INTRODUCTION

Impulse friction stir welding (IFSW) has been developed and patented in 2001 [1]. Like in the traditional friction stir welding (FSW), IFSW joins materials in a solid condition, which preserves all the advantages of FSW in IFSW joints [2]. These processes are commonly applied in the production of light structures from aluminum alloys used in various fields of engineering [3, 4].

A principal feature distinguishing IFSW from FSW is the fact that the axial force acting on the material during the impulse process is not constant. As a result, the friction force, the torque, the contact conditions on the tool/billet interface, and the thermal power vary during the welding process. The main advantage of IFSW is elevation of the mechanical properties of the welded joint above those of the matrix metal. An additional pulse imposed during the welding raises the level of plastic strain in the material and thus promotes refinement of the structure of the weld. This affects positively the mechanical properties of the welded joint, especially the fatigue resistance [1]. It has been shown in [5] that the endurance of welded joints of aluminum-magnesium alloy 6082-T6 after IFSW is 40% higher than after the traditional FSW.

It is known that the oxide layer formed under FSW on the interface of two parts of a welded joint fractures during the tool welding and is transferred to the region of the weld [6 – 12]. The oxide blisters retained in the welded joints consist of mall-size particles of Al_2O_3 (< 100 nm) forming dense accumulations negatively affecting the strength and fatigue properties of the welded joint. It has been shown in [9] that the fatigue resistance of welded joints of aluminum alloys 5058 and 2024 containing oxide inclusions is 35 and 55% lower, respectively, than that of the welded joints bearing no oxide inclusions (after 2×10^6 loading cycles). By the data of [7], the distribution of the oxide layer affects considerably the ultimate strength and the elongation of aluminum alloys.

Precipitation hardening of alloy 6082 is a result of precipitation of intermetallic phases from the solid solution. The process involves precipitation and growth of an equilibrium Mg_2Si β-phase, its intermediate phases and clusters in the aluminum matrix. By the data of [13, 14], alloy 6082 contains intermetallic inclusions of different compositions and sizes, i.e., coarse (1 – 10 μm) and very fine (0.1 – 1 μm) particles, in addition to the equilibrium β-Mg_2Si phase. Addition of copper into an Al – Mg – Si alloy promotes formation of a *Q*-phase, which affects positively the kinetics of artificial aging [15]. A study of these phases in the structure of a friction stir welded joint has shown the presence of four regions with specific distributions of the particles of the hard-

[1] St. Petersburg Polytechnic University, St. Petersburg, Russia (e-mail: petroprom2013@yandex.ru).
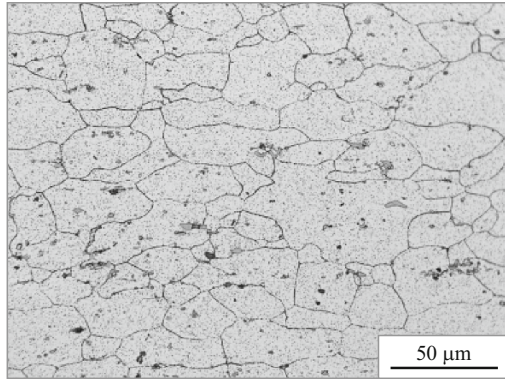[2] Brandenburg University of Technology, Cottbus, Germany.

Fig. 1. Structure of the base metal (alloy 6082-T6).

ening phase (the size, the density, the morphology). The differences are a result of the action of different maximum temperatures in different regions of the weld in the welding process [16]. It has been shown in [17, 18] that increase in the power of the heat introduced during FSW into Al – Mg – Si alloys causes growth of a stable Q-phase and formation of dispersed Al – Mg – Si intermetallics in the zone of dynamic recrystallization and of a metastable four-component Q'-phase in the thermomechanically affected zone, which worsens the strength properties.

The aim of the present work was to determine the effect of the force and frequency of a friction stir welding pulse on the microstructure (the grain size, the distribution of the oxide layer and of the particles of the hardening phase) and mechanical properties (the hardness, the strength, the ductility) of a welded joint of an aluminum alloy of the Al – Mg – Si system.

METHODS OF STUDY

We applied impulse and traditional friction stir welding to sheets with a size of 125×400 mm and a thickness 2 mm from aluminum alloy 6082 in state T6. The alloy had the following chemical composition in wt.%: 0.89 Si, 0.40 Fe, 0.31 Cu, 0.40 Mn, 1.18 Mg, the remainder Al. The mechanical properties of the base metal were as follows: $\sigma_r = 323$ MPa; $\sigma_{0.2} = 257$ MPa; $\delta = 6.3\%$.

The structure of the base metal in the state as delivered contains grains extended in the rolling direction (about 38 mm in the longitudinal direction and about 20 μm in the transverse direction) (Fig. 1).

Friction stir welding was conducted in a triaxial miller equipped with a special tool and a hydraulic system providing rotation and motion of the tool with simultaneous feeding of pulses; the cylindrical tip had a diameter of 4 mm and the shoulder had a diameter of 12.5 mm. In the process of FSW the tool was immersed into the material to a depth of 1.8 mm. The plates were pressed by massive grips to the steel substrate at a minimum distance between them. The FSW parameters were as follows: welding speed 400 mm/min, speed of rotation of the tool 710 rpm, angle of slope of the axis of the tool 2°. The parameters of the IFSW process are given in Table 1.

We performed a metallographic analysis for determining the regions (zones) of the welded joints and studying the microstructure. The samples for the light microscopy were prepared by color etching using a reagent containing 1 g NaOH, 4 g $KMnO_4$, and 100 ml H_2O. The microstructure of the base metal and of the zones of the weld was studied using a Leica DM 2500 M light microscope at a magnification of up to $\times 500$. The grain size was determined automatically with the help of the QX-Grain software in the zones of dynamic recrystallization, thermomechanical effect and heat effect, and in the base metal. The microstructure was also studied with the help of a MIRA II XMH Tescan scanning electron microscope at the following parameters: voltage 15 kV, accelerating voltage 124.4 eV, angle of deflection 40.6°. The microscopic x-ray spectrum analysis of inclusions of the hardening phase was conducted using an INCA Oxford spectrometer (50 mm^2) attached to the microscope.

The Vickers hardness was measured over the line passing at a distance of 1.1 mm from the lower surface of the weld at a load of 0.9807 N applied for 15 sec. The transverse specimens with rectangular section were tested for tensile strength using a Walter + bai AG universal machine at a loading speed of 1.2 mm/min until breakage of the specimen. Two spring clips were mounted on the specimen so that the distance between them was 50 mm.

TABLE 1. Parameters of Welding Processes, Characteristics of Hardening Phase in DRZ and Mechanical Properties of Welded Joints of Alloy 6082-T6

Specimen	Kind of welding	I, kN	f, Hz	V, vol.%	d_{av}, μm	σ_r, MPa	$\sigma_{0.2}$, MPa	δ, %
A	FSW	0	0	3.12	1.28	235	175	1.0
B	IFSW	1.0	8.9	2.23	1.17	248	170	2.1
C	IFSW	2.5	8.9	2.74	1.3	205	161	1.3
D	IFSW	10.0	5.9	3.34	1.34	193	158	1.2

Notations: FSW and IFSW) transitional and impulse friction stir welding, respectively; I) pulse intensity; f) pulse frequency; V) volume fraction of hardening phase in the zone of dynamic recrystallization (DRZ); d_{av}) average phase diameter; σ_r) ultimate strength; $\sigma_{0.2}$) yield strength; δ) elongation.
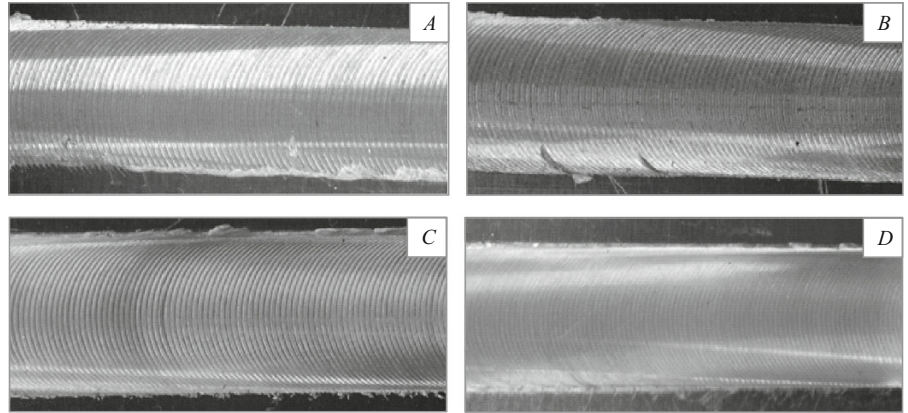
Fig. 2. Surfaces of welded joints from alloy 6082-T6 after FSW (specimen *A*) and after IFSW (specimens *B*, *C* and *D*).

RESULTS

Figure 2 presents the surfaces of the welded joints formed by FSW and IFSW under the shoulders of the tool. It can be seen that feeding of a pulse during the FSW changes the appearance of the weld. When the pulse intensity is increased, the sizes of the flakes grow, while increase in the frequency of the pulse increases their number. Increase in the pulse intensity to 10 kN produces a sheet-thinning defect as a result of knocking-off of the material in the welding process. We detected no other defects on the upper and lower surfaces of the welded joint.

Analyzing the structure of a cross section of the weld formed by IFSW (Fig. 3) we detected the same zones (regions) as in the joint formed by FSW. The zone of dynamic recrystallization (DRZ) was located in the center of the cross section and had a fine-grained structure. Under the action of severe plastic deformation and high temperature the thermomechanically affected zone (TMAZ) acquired a strained structure. The heat-affected zone (HAZ) of the structure was coarse-grained, because the material in this zone had experienced a purely thermal action. Note that in contrast to the FSW, the DRZ and the TMAZ became narrower and changed under the IFSW.

The study of the macro- and microstructures in cross sections of the welded joints formed by FSW and IFSW has shown that the oxides getting into the joint under impulse welding are more refined and more uniformly distributed in the structure (Fig. 4). After the FSW the oxide layer remains in the DRZ in the form of a wavy band, whereas after the IFSW it is distributed in the form of fine oxide particles. Increase in the pulse intensity under the IFSW intensifies this effect due to higher straining of the metal, which should affect positively the mechanical properties of the weld [16].

The results of the study of the microstructure in the DRZ reflect formation of fine equiaxed grains of matrix α-solid solution after the IFSW (Fig. 5), like under the FSW [18 – 21]. Figure 6 presents the variation of the grain size in the DRZ, TMAZ and HAZ of welded joints depending on the parameters of the used IFSW. At a low pulse intensity, the grain size
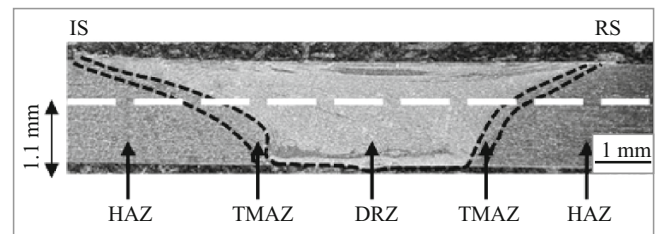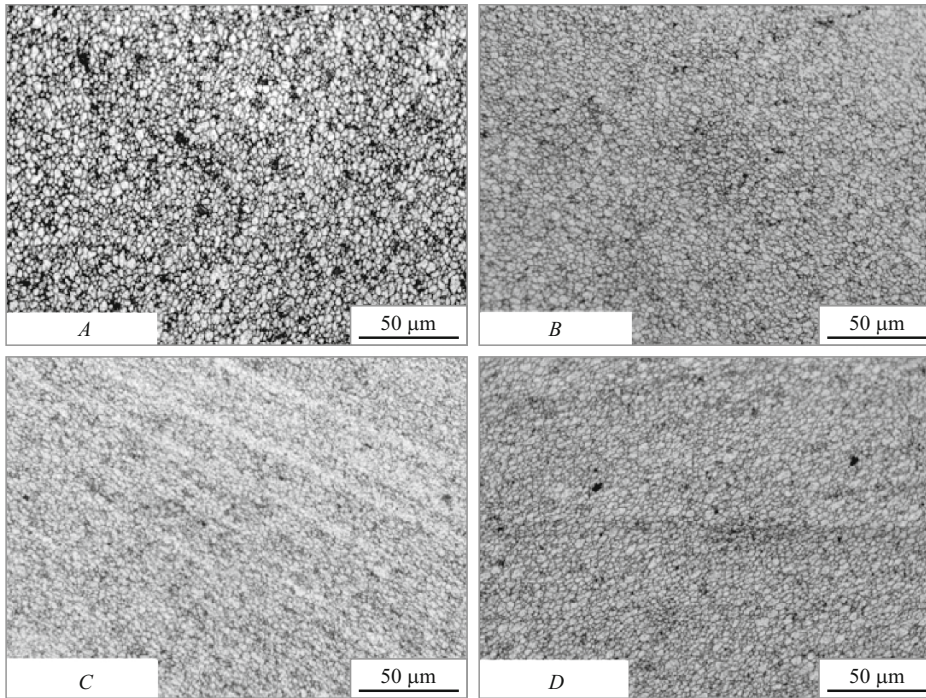

Fig. 3. Macrostructure of a welded joint of alloy 6082-T6 in cross section after IFSW: IS and RS) invasion and retreat sides; HAZ and TMAZ) heat-affected and thermomechanically affected zones, respectively; DRZ) dynamic recrystallization zone.
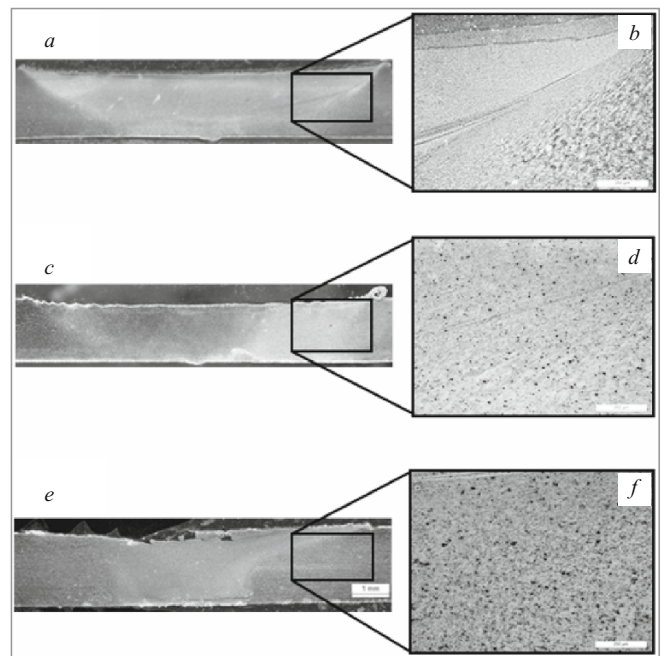
Fig. 4. Macrostructure of the weld in cross section of IFSW joint (*a*, *c*, *e*) and microstructure of the singled out regions (*b*, *d*, *f*): *a*, *b*) specimen *A*; *c*, *d*) specimen *B*; *e*, *f*) specimen *C*.

ranges within 2.5 – 3.0 µm. At a constant pulse frequency, the grain size decreases with growth in the pulse intensity to
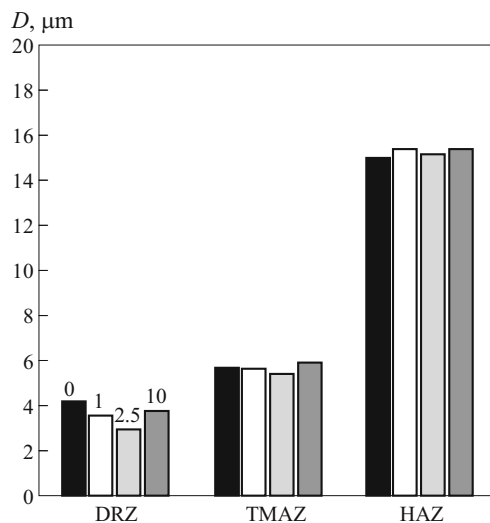
Fig. 5. Structure of a welded joint of alloy 6082-T6 in the region of dynamic recrystallization after FSW (specimen *A*) and IFSW (specimens *B*, *C*, *D*).

2.5 kN; at a pulse intensity of 10 kN it increases to about 3.7 μm. The average grain size in the TMAZ and HAZ differs inconsiderably both for the FSW and for the IFSW. Note that after the IFSW at a low pulse intensity (1 – 2.5 kN), the grain size in the DRZ is smaller than after the FSW.

Figure 7 presents the distribution of hardening phases in the structure of DRZ after FSW and IFSW. It can be seen that these phases have the form of light coarse inclusions of an irregular extended shape with a size of 1 – 5 μm. The x-ray spectrum microanalysis has shown that the hardening parti-

cles in the DRZ are unlike inclusions with different concentrations of Si, Mn, Mg, Fe and Cu. The chemical compositions and the sizes and shapes of the inclusions allow us to speak of the presence of intermetallic particles of AlFe(Mn)Si, a β-phase (Mg_2Si) and/or a *Q*-phase (of the Al – Mg – Si – Cu system) in the DRZ. The parameters of the particles

Fig. 6. Grain size of a welded joint of alloy 6082-T6 after IFSW at different pulse intensities (given at the columns in kN): DRZ) dynamic recrystallization zone; TMAZ) thermomechanically affected zone; HAZ) heat-affected zone.
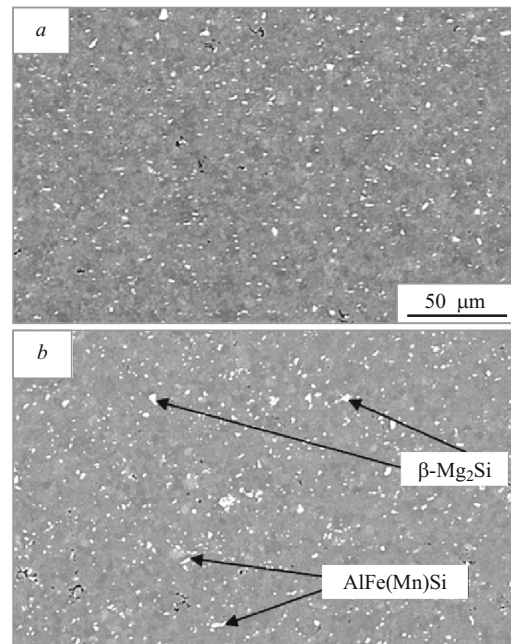
Fig. 7. Structure of the dynamic recrystallization zone in a welded joint of alloy 6082-T6 (electron microscope): *a*) specimen *A*, FSW; *b*) specimen *B*, IFSW.
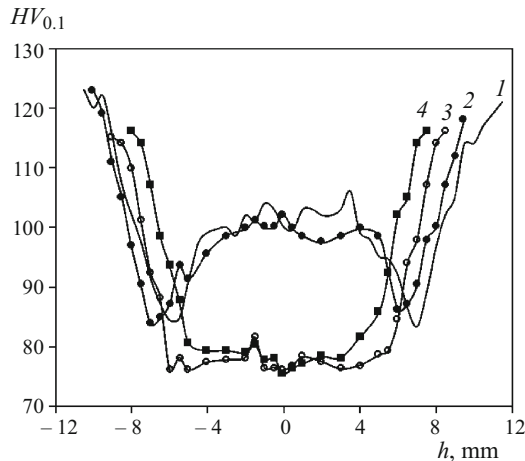
Fig. 8. Distribution of microhardness $HV_{0.1}$ in welded joints of alloy 6082-T6 after FSW and IFSW (h is the distance from the center of the weld): *1*) 0 kN; *2*) 1.0 kN, 8.9 Hz; *3*) 2.5 kN, 8.9 Hz; *4*) 10.0 kN, 5.9 Hz.

of the hardening phases in the DRZ of the FSW and IFSW joints are presented in Table 1. It follows from the Table that the volume fraction and the average size of the particles of hardening phases in the DRZ of the joints formed by IFSW with a low pulse (below 1 kN) are lower than after the FSW. Increase in the pulse intensity of the IFSW to 10 kN causes considerable growth in the volume fraction of coarse particles and growth of stable phases and intermetallics of the Al – (Fe(Mn) – Si system in the structure of the alloy.

The results of the measurement of microhardness of welded joints are presented in Fig. 8. It has been shown in [14, 22] that heat-hardened aluminum alloys exhibit *W*-shape curves of distribution of microhardness over cross sections of welds. A profile of such a shape contains a plateau in the center of the weld, the width of which commonly corresponds to the width of the shoulders. With distance from the center of the weld the hardness decreases to a minimum value in the HAZ and then grows to the hardness of the base metal. In our work we obtained similar curves of hardness distribution in the welds formed by FSW and IFSW with low pulse intensity (1 kN). The hardness of the base metal is about 120 $HV_{0.2}$ and decreases from the edge to the center of the weld (to about 80 $HV_{0.1}$). The lowest hardness value has been detected in the HAZ at a distance of 6 – 7 mm from the

center of the weld. The results show that the pulse parameters in the IFSW affect considerably the hardness in the DRZ. The highest hardness has been obtained in the welded joints formed at a low pulse intensity (up to 1 kN) and amounts to 97 – 100 $HV_{0.1}$ (79% of the hardness of the base metal). Under the IFSW with a higher pulse intensity the hardness in the DRZ is 36% lower than that of the base metal.

The results of the tensile tests of FSW and IFSW joints are presented in the Table. Comparative analysis shows considerable increase in the ultimate strength and elongation and some decrease in the yield strength of the welded joints formed by the IFSW as compared to the same characteristics after the FSW. However, further increase in the pulse intensity is accompanied by decrease in the strength and ductility parameters of the joints, which may be caused by a sheet-thinning defect. In the joints welded at 1 kN and 8.9 Hz the place of failure is located in the HAZ on the side of invasion, whereas the other specimens fail over the joining line, i.e., in the zone of dynamic recrystallization (Fig. 9).

CONCLUSIONS

1. The structure of the welded joints of sheets of aluminum alloy 6082-T6 (of the Al – Mg – Si system) produced by impulse friction stir welding contains three regions typical for the traditional friction stir welding. However, application of a pulse reduces the width of the zones of dynamic recrystallization and thermomechanical effect in the welded joint.

2. The oxide layer is stirred more efficiently in the joints formed by IFSW than in the case of FSW.

3. Application of a pulse promotes refinement of the structure of the welded joint, especially in the zone of dynamic recrystallization, due to the action of additional plastic strain during the friction stir welding.

4. The parameters of the IFSW process affect substantially the kind of the structure of the welded joint of the aluminum alloy including the sizes and the distribution of the particles of the hardening phases.
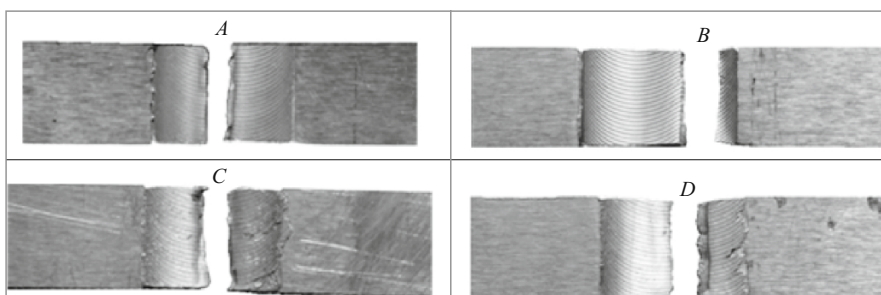
Fig. 9. Appearance of specimens *A* – *D* after tensile tests until failure of welded joints of alloy 6082-T6 produced by FSW and IFSW.

REFERENCES

1. V. Michailov, *Impuls-Rührreibschweißen (Impulse Friction Stir Welding)*, DE 199 53 260.5.

2. W. M. Thomas, E. D. Nicholas, J. C. Needham, et al., *International Patent Application No. PCT/GB92/02203, GB Patent Application No. 9125978.8* (1991).

3. S. Yu. Kondrat'ev and O. V. Shvetsov, "Effect of high-temperature heating on the structure and properties of aluminum alloys in the production of drill pipes," *Metal Sci. Heat Treat.*, **55**(3 – 4), 191 – 196 (2013).

4. S. Yu. Kondrat'ev, O. G. Zotov, and O. V. Shvetsov, "Structural stability and variation of properties of aluminum alloys D16 and 1953 in the production and operation of drill pipes," *Metal Sci. Heat Treat.*, **55**(9 – 10), 526 – 532 (2014).

5. V. Michailov, C. Hantelmann, and A. Kloshek, "Impuls-rührreibschweißen — Ein Verfahren mit neuen Möglichkeiten," in: *Große Schweißtechnische Tagung*, DVS Band 275 (2011), pp. 171 – 176.

6. R. S. Mishra and Z. Y. Ma, "Friction stir welding and processing," *Mater. Sci. Eng. R: Reports*, **50**(1 – 2), 1 – 78 (2005).

7. P. Niu, W. Li, Z. Zhang, et al., "Significant effect of oxide on mechanical properties of friction-stir welded AA2024 joints," *Sci. Technol. Weld. Join.*, **22**, 66 – 70 (2016).

8. Y. S. Sato, F. Yamashita, Y. Sugiura, et al., "FIB-assisted TEM study of an oxide array in the root of a friction stir welded aluminum alloy," *Scr. Mater.*, **50**, 365 – 369 (2004).

9. C. Zhou, X. Yang, and G. Luan, "Effect of oxide array on the fatigue property of friction stir welds," *Scr. Mater.*, **54**, 1515 – 1520 (2006).

10. T. Le. Jolu, T. F. Morgeneyer, and A. F. Gourgues-Lorenzon, "Effect of joint line remnant on fatigue lifetime of friction stir welded Al – Cu – Li alloy," *Sci. Technol. Weld. Join.*, **15**, 694 – 698 (2010).

11. Y. S. Sato, H. Takauchi, S. H. C. Park, and H. Kokawa, "Characteristics of the kissing-bond in friction stir welded Al alloy 1050," *Mater. Sci. Eng. A*, **405**, 333 – 338 (2005).

12. H. J. Liu, H. J. Liu, Y. C. Chen, and J. C. Feng, "Effect of zigzag line on the mechanical properties of friction stir welded joints of an Al – Cu alloy," *Scr. Mater.*, **55**, 231 – 234 (2006).

13. L.-E. Svensson, L. Karlsson, H. Larsson, et al., "Microstructure and mechanical properties of friction stir welded aluminum alloys with special reference to AA5083 and AA6082," *Sci. Technol. Weld. Join.*, **5**, 285 – 296 (2000).

14. L. Karlsson, L.-E. Svensson, and H. Larsson, in: *Proc. 5th Int. Conf. on Trends in Welding Research, Pine Mountain, GA, USA, June 1 – 5*, ASM Int. (1998), pp. 574 – 579.

15. W. F. Mao and D. E. Laughlin, "Effects of Cu content and preaging on precipitation characteristics in aluminum alloy 6062," *Metall. Mater. Trans. A*, **31A**, 361 – 371 (2000).

16. Y. S. Sato, H. Kokawa, M. Enomoto, and S. Jogan, "Microstructural evolution of 6063 aluminum during friction-stir welding," *Metall. Mater. Trans. A*, **30A**, 2429 – 2437 (1999).

17. C. A. W. Olea, L. Roldo, J. F. dos Santos, and T. R. A. Strohaecker, "A sub-structural analysis of friction stir welded joints in an AA6056 Al-alloy in T4 and T6 temper conditions," **454 – 455**, 52 – 62 (2007).

18. C. A. Weis Olea, *Influence of Energy Input in Friction Stir Welding on Structure Evolution and Mechanical Behavior of Precipitation-Hardening in Aluminum Alloys (AA2024-T351, AA6013-T6 and Al – Mg – Sc)* (2008).

19. Kh. A. A. Hassan, P. B. Prangnell, A. Norman, et al., "Effect of welding parameters on nugget zone microstructure and properties in high strength aluminum alloy friction stir welds," *Sci. Technol. Weld. Join.*, **8**, 257 – 268 (2003).

20. W. B. Lee, Y. M. Yeon, and S. B. Jung, "Evaluation of the microstructure and mechanical properties of friction stir welded 6005 aluminum alloy," *Mater. Sci. Technol.*, **19**, 513 – 518 (2003).

21. C. Genevois, A. Deschamps, A. Denquin, and B. Doisneaucottignies, "Quantitative investigation of precipitation and mechanical behavior for AA2024 friction stir welds," *Acta Mater.*, **53**, 2447 – 2458 (2005).

22. P. L. Threagill. A. J. Leonard, H. R. Shercliff, and P. J. Withers, "Friction stir welding of aluminum alloys," *Int. Mater. Rev.*, **54**(2), 49 – 93 (2009).